



ELSEVIER

Applied Mathematics and Computation 129 (2002) 55–85

APPLIED  
MATHEMATICS  
AND  
COMPUTATION

www.elsevier.com/locate/amc

# Computational explorations into the dynamics of rings of coupled oscillators

Hubertus F. von Bremen, Firdaus E. Udwardia <sup>\*,1</sup>

*Department of Aerospace and Mechanical Engineering, University of Southern California,  
Los Angeles, CA 90089-1453, USA*

---

## Abstract

This paper deals with the response of homogeneous and inhomogeneous rings of coupled oscillators where each individual oscillator, when uncoupled from the others, is chaotic. It is shown that coupling can bring about a wide variety of global responses, and that there is a significant range of coupling values when the response of the ring is periodic despite the fact that each oscillator is chaotic. In fact numerous periodic solutions can be found depending on the initial conditions. The response of a coupled set of homogeneous and non-homogeneous rings is also investigated showing that the behavior of such coupled compartmental models can be quite counterintuitive and sensitive to the parameters that describe the extent and nature of coupling. © 2002 Elsevier Science Inc. All rights reserved.

*Keywords:* Rings of coupled chaotic oscillators; Homogeneous and inhomogeneous rings; Compartmental dynamics; Multiple attractors

---

## 1. Introduction

The global behavior of a large collection of elemental ‘units’ or ‘agents’ each of which interacts only with its local neighbors is a crucial question for mathematicians, physicists, biologists, ecologists, sociologists, and economists. Perhaps the most fascinating example of the emergence of global patterns

---

\* Corresponding author.

*E-mail address:* fudwadia@usc.edu (F.E. Udwardia).

<sup>1</sup> Also at Information and Operations Management, and Mathematics, 430K Olin Hall of Engineering, University of Southern California, Los Angeles, CA 90089-1453, USA.

through local interactions is that of the brain, where it is not easy to understand how the poorly correlated activity of individual neurons generates macroscopic, collective activity, as measured, for example, in EEGs.

Even though this might appear as a classical problem in physics, where, as in kinetic theory, one is interested in the determination of the behavior at the macroscopic level of a large ensemble of molecules (units), each colliding with one another, it is only recently that this problem has begun to be considered in greater generality, where the individual units exhibit more complex and nonlinear interactions with their local neighbors. This is mainly due to the advent of computers without which it would be impossible to explore the behavior of such complex systems, since the presently available analytical techniques are inadequate for handling general, large-scale, nonlinear, dynamical systems. Of particular interest are systems in which the individual units interact in a simple fashion without being subjected to any ‘centralized’ control. And yet, even when the individual units show chaotic behavior, they are often somehow able to ‘organize’ themselves to produce nontrivial global responses – responses that are not simple reproductions or superpositions of the many chaotic disordered responses of each of the units.

This paper deals with computational explorations into the dynamics of coupled nonlinear systems where each of the individual units is chaotic in nature. Furthermore, we specialize our investigation to *rings* of such elemental units. Ring geometries arise extensively in the modeling of chemical, physiological, and biochemical systems. Starting with the seminal work of Turing [1], who analyzed rings of cells as models of morphogenesis and proposed that isolated rings could account for the tentacles of the hydra, ring geometries have been utilized in many situations – for example, the study of: slow-wave activity in the mammalian intestine [2], oscillatory behavior of three coupled neurons [3], locomotor central pattern generation [4–6], neural network theory [7], development of patterns on certain animal shells and the function of smooth muscle systems [8]. Experimental observations of dynamical behavior of rings of 4, 5 and 6 oscillators related to the B–Z reaction were reported by Nishiyama [9]. Rotating waves in rings of coupled periodic oscillators have been observed by Matias [10]. A group-theoretic approach to rings of coupled biological oscillators was developed by Collins and Stewart [11]. Several papers on coupled map lattices can be found in [12].

From a mathematical standpoint several techniques have been employed to bring about partial understanding of the global behavior of units that are connected together in ring geometries. The methods often employed are harmonic balance [2], nonlinear mode analysis [13], phase-transition diagrams [14], perturbation methods and stability theory [8], qualitative methods [15], and numerical simulations [16]. However, most of these analytical studies are limited to the exploration of certain special systems and/or special features of

these systems, and they usually deal with a small number of interacting units, typically less than 7 or 8 [16].

The study reported in this paper was motivated by two central questions: (1) What is the type of dynamical behavior that can be generated by a ring of coupled chaotic oscillators, (2) What is the type of compound behavior of a dynamical system consisting of two rings of chaotic oscillators, or compartments, each interacting with the other. Our computational explorations into these aspects (see [17]), we believe, provide abundant surprises and open up new questions that need further investigation both analytically (so far as that may be possible) and simulation-wise. To the best of our knowledge, such explorations have so far not been reported on rings containing several tens of chaotic oscillators. We hope that theoreticians will be motivated to explain some of the behavior which we computationally observe.

The organization of the paper is as follows. Section 2 provides the basic model for the ring of nonlinear oscillators (units) that we shall consider. Section 3 shows the dynamical behavior of the ring with explorations into the influence of various initial conditions. Computational results with rings of identical individual units as well as rings with non-identical units are illustrated. Section 4 shows the behavior of the interaction of two rings. In Section 5 we provide our conclusions, point to some possible areas of applications where these results may be useful, and indicate some of the questions that remain unanswered.

## 2. Model of a single ring of oscillators

Consider a ring consisting of  $n$  oscillators (units), each connected to its nearest neighbor. We let the evolution of the  $j$ th oscillator be given by the following iterative equation:

$$x_j(i+1) = bf(x_{j-1}(i), \alpha_{j-1}) + af(x_j(i), \alpha_j) + bf(x_{j+1}(i), \alpha_{j+1}), \quad (1)$$

with  $f(x, \alpha) = 1 - \alpha x^2$ .

That is, the response of the  $j$ th oscillator at the  $(i+1)$ th iteration is a function of the response of the  $j$ th oscillator and its two neighboring oscillators at the  $i$ th iteration. Due to the closing of the ring, the response of  $x_1(i+1)$  depends on  $x_1(i)$ ,  $x_2(i)$  and  $x_n(i)$ , and similarly the response of  $x_n(i+1)$ . See Fig. 1 for a schematic depiction of the system. Each oscillator may be thought of as located at one of the  $n$  ‘nodes’ of the ring, and we shall at times refer to these oscillators, and their responses, simply by their node numbers.

The dynamical system described in (1) can also be expressed as

$$x(i+1) = A\tilde{f}(x(i), \alpha), \quad (2)$$

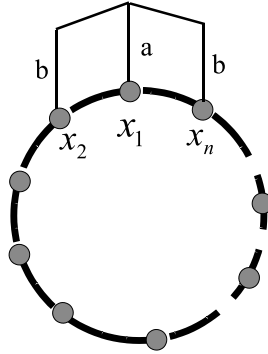


Fig. 1. Ring of oscillators.

where  $\alpha$  and  $x$  are vectors of length  $n$ , the  $n \times n$  matrix  $A$  is given by

$$A = \begin{bmatrix} a & b & & & b \\ b & a & b & & \\ & b & a & b & \\ & & & \ddots & \\ b & & & & b \\ & & & & b & a \end{bmatrix}, \quad (3)$$

and

$$\begin{aligned} \tilde{f}(x(i), \alpha) &= [f(x_1(i), \alpha_1) \quad f(x_2(i), \alpha_2) \quad f(x_3(i), \alpha_3) \quad \cdots \quad f(x_n(i), \alpha_n)]^T \\ &= [1 - \alpha_1 x_1^2(i) \quad 1 - \alpha_2 x_2^2(i) \quad 1 - \alpha_3 x_3^2(i) \quad \cdots \quad 1 - \alpha_n x_n^2(i)]^T. \end{aligned}$$

In this paper we shall assume that  $a + 2b = 1$ . When there is no coupling between the oscillators (i.e.  $b = 0$ ,  $a = 1$ ), we have  $n$  independent oscillators. In this case the evolution of the  $j$ th oscillator is simply given by the equation

$$x_j(i+1) = 1 - \alpha_j (x_j(i))^2. \quad (4)$$

Fig. 2 shows a bifurcation plot for the scalar function  $f(x, \alpha) = 1 - \alpha x^2$ . From the bifurcation plot we can observe the ranges in  $\alpha$  which will lead to periodic solutions of (4), and also the regions where we expect chaotic solutions of (4).

### 3. Effect of initial conditions on the response of a single ring

In this section we explore the behavior of the oscillator-ring presented in Section 2 and show that such rings can exhibit a wide range of dynamical behavior depending on the choice of parameter values and initial conditions. In

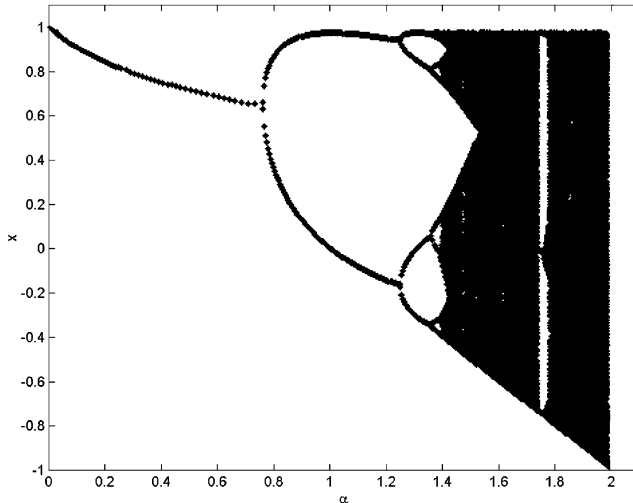


Fig. 2. Bifurcation plot of  $f(x, \alpha) = 1 - \alpha x^2$ .

the first part of this section we consider a ring ( $n = 32$ ) of identical chaotic oscillators. Depending on the choice of initial conditions and the parameter  $b$  that describes the local interactions between the oscillators, we show that the system exhibits a wide variety of global asymptotic behaviors. For example we show the existence of several stable periodic solutions (when  $b = 0.2$  and  $\alpha = 1.9$ ), each solution having the *same* period, depending on the choice of initial conditions. In the second part of the section, we show that rings of non-identical oscillators, can have several different attractors, structurally different in general, depending on the choice of initial conditions.

### 3.1. A ring of identical oscillators

The evolution of the dynamics of the ring of oscillators as described by Eq. (2) with parameter values of  $a = 0.6$ ,  $b = 0.2$ , and  $\alpha_j = 1.9 \forall j$ , is computationally studied. Each oscillator when decoupled from its neighbors exhibits a chaotic response characterized by a positive Lyapunov Exponent of 0.549. However, depending on the choice of initial conditions, we observe that the coupled oscillator-ring system reaches different periodic solutions (each periodic solution with period 4). In all our computer experiments, the system's response initially appears chaotic. It is only after the system is allowed to evolve for a considerable number of iterations that a periodic response emerges, a phenomenon similar to perturbation. In each case our experiments show that the transition to periodic behavior occurs over a remarkably short

number of iterations, though. The periodic solutions computationally found are shown to be stable solutions, as expected. First we show the typical evolution of the system for a given set of initial conditions, and then we present a set of initial conditions that lead to *different* periodic solutions, *each* of period 4.

The numerical computations were performed using MATLAB. Uniformly distributed random numbers were used to generate the initial conditions. By changing the value of the seed,  $s$ , of the random number generator, different initial conditions were obtained. In MATLAB code, the initial condition  $n$ -vector,  $x_i$ , was generated using the commands: `rand('seed', s)`; and  $x_i = \text{rand}(n, 1) - 0.5$ .

Typical behavior of the first component of the  $n$ -vector  $x$  ( $n = 32$ ), is shown in Fig. 3. The initial conditions correspond to random numbers generated using a seed value,  $s = 1$ . It is clear from the figure that initially this response covers a wide range of values. After a considerable number of iterations (about 190,000, in this case) the response evolves to a periodic solution. It is worth noting (see Fig. 3) that though the periodic solution emerges after  $O(10^5)$  iterations, the transition to a periodic solution occurs rather abruptly over a relatively small number of iterations of only  $O(10^2)$ .

The projections of the values of the responses of the oscillators (from iteration numbers 195,000–196,000) at each of the 32 nodes are shown in Fig. 4. The figure clearly shows that each node only attains at most 4 values, an indication that the solution is possibly periodic.

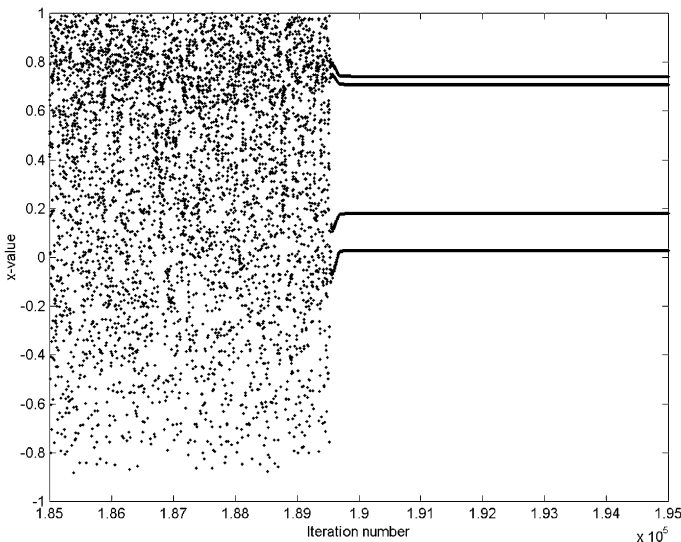


Fig. 3. Time evolution of the first node, when using a seed  $s = 1$  for the initial conditions.

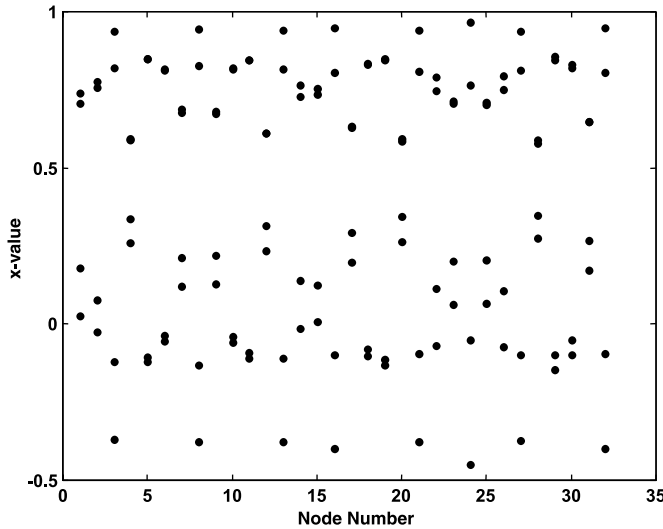


Fig. 4. Projection of the solutions from iteration number 195,000 to 196,000, when using a seed  $s = 1$  for the initial conditions.

Eq. (2) is basically a map  $h : R^n \rightarrow R^n$ , where  $h(x)$  for  $x \in R^n$  is given by

$$h(x) = A\tilde{f}(x, \alpha). \tag{5}$$

A point  $p$  is a periodic fixed point of  $h$  with period  $k$  if  $h^k(p) = p$ , and  $h^j(p) \neq p$  for  $0 < j < k$ .

The 4-period solution of the ring is shown in Fig. 5. In this figure,  $p$  corresponds to the state of the oscillator-ring after 2,000,000 iterations. The circles show the locations of the oscillators in the ring. The solid large dot indicates node 8 and the solid small dot indicates node 24, the node numbers increasing in the counterclockwise direction. The response of each oscillator is depicted by the vertical line that ends in a diamond. Though at first sight the response appears to be symmetric about the axis joining nodes 8 and 24, closer examination shows that it is in fact not so.

Similar dynamical behavior is found when different seed values ( $s$  ranging from 1 to 20) for the random number generator are used; each seed value,  $s$ , provides a corresponding random initial condition for the dynamical system of equation (2). Each initial condition investigated in this study produces, asymptotically, a 4-period solution; the number of iterations required for the periodic solution to emerge in each case is different, though. As before, in all the cases explored, the system initially has a response which seems chaotic (the solutions span a wide range of values in a non-apparent pattern). Eventually the system settles to a periodic solution. For each seed value used, the com-

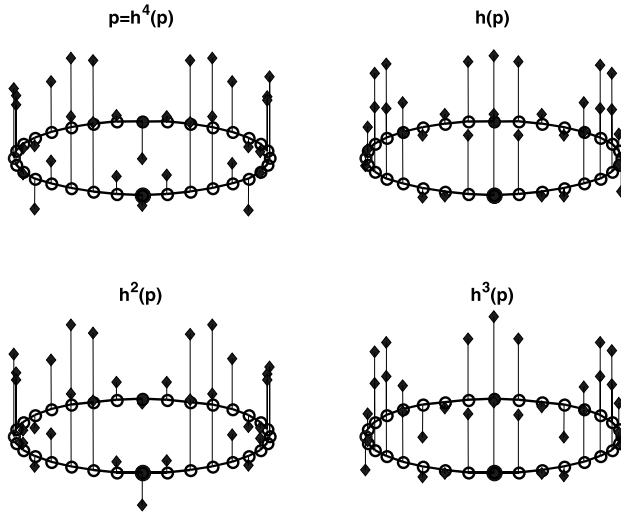


Fig. 5. Periodic solution using a seed,  $s = 1$ .

ponent-wise difference,  $p - h^4(p)$ , (with  $p$  corresponding to the state of the dynamical system, Eq. (2), at iteration number 2,000,000) is within the order of the machine precision ( $\text{eps} \approx 2.22 \times 10^{-16}$ ).

Table 1 shows the largest five Lyapunov characteristic exponents<sup>2</sup> (LCEs) computed for the system when seeds of 1, 5, 10, 14 and 16 are used to generate sets of random initial conditions. In each case the system is allowed to evolve for 2,000,000 iterations; the next 50,000 iterations are then used to compute the LCEs shown in the table. The fact that all the LCEs are negative, confirms that the solution is not chaotic for each of the cases considered. In fact, as observed before, all the solutions are periodic (with period 4).

The stability of the fixed point  $p$  can be established by looking at the magnitude of the eigenvalues of the Jacobian map,  $Dh^k(p)$ . Table 1 also shows the largest five magnitudes of the eigenvalues of the Jacobian,  $Dh^k(p)$ , where  $p$  is the state of the dynamical system at iteration number 2,000,000. Since the moduli of these eigenvalues are all less than unity, this again confirms that for each initial condition considered, the periodic fixed-points  $p$  are asymptotically stable. Having established that these 4-period solutions recurrently appear for every initial condition that was considered, the next question is obviously if they are all the same.

<sup>2</sup> See [18] for the stable and efficient method to compute all the LCEs, and [19] for the computation of just the largest  $p$  LCEs.

Table 1  
Largest five LCEs and largest five magnitudes of the eigenvalues of  $Dh^k(p)$  when using seed values,  $s$ , of 1, 5, 10, 14 and 16 to generate the initial condition

Seed = 1		Seed = 5		Seed = 10	
LCEs	$ \text{eig}(Dh^4(p)) $	LCEs	$ \text{eig}(Dh^4(p)) $	LCEs	$ \text{eig}(Dh^4(p)) $
-0.0232	0.9116	-0.0228	0.9129	-0.0293	0.8897
-0.0436	0.8402	-0.0467	0.8298	-0.0547	0.8038
-0.0537	0.8068	-0.0578	0.7939	-0.0595	0.7880
-0.0916	0.6933	-0.0912	0.6945	-0.0832	0.7171
-0.0916	0.6933	-0.0911	0.6945	-0.0833	0.7171
Seed = 14		Seed = 16			
-0.0357	0.8669	-0.0058	0.9771		
-0.0537	0.8070	-0.0059	0.9771		
-0.0537	0.8070	-0.0098	0.9616		
-0.0820	0.7207	-0.0347	0.8708		
-0.1071	0.6515	-0.0584	0.7918		

One way to determine if two periodic solutions of a ring of oscillators generated from two different initial conditions are the same, is to compare one solution of the ring against all possible ‘rotations’ of the other solution. This process requires the consideration of many cases, and may be computationally somewhat time consuming. When comparing two periodic solutions of a ring of oscillators, if there exists at least one value that is achieved by one of the solutions and not by any of the oscillators of the other solution, then it is clear that the two periodic solutions are different. This leads to a simple and quick way to show that two periodic solutions are different without having to consider the rotations of one solution, as shown in Fig. 6. The figure shows all the values the system achieves (values within a tolerance of  $10^{-8}$  are shown) in ascending order after the system has settled to a periodic solution for different initial conditions. Since there is no complete overlap in the possible values reached among the periodic solutions obtained from different seed values, the periodic solutions must be different.

The periodic solutions shown in Fig. 6 reflect that there are a total of 128 possible positions for the oscillators in the ring for each of the three different seed values shown. In this case, each oscillator has 4 possible values and no oscillator shares its locations with any other oscillator (that is why we have  $128 = 4 \times 32$  possible values). Among the cases we explored, we also found several 4-period solutions with 64 possible values. Here, the solution is symmetric on the ring (see [11]). As an example of this behavior, Fig. 7 shows the projections of the responses of the oscillators for every node using random initial conditions generated with a seed of 5. The projections shown correspond to positions of the oscillators from the iteration number 2,000,000–2,005,000. By focusing on node 8, we can see that the projection of the response of node 7

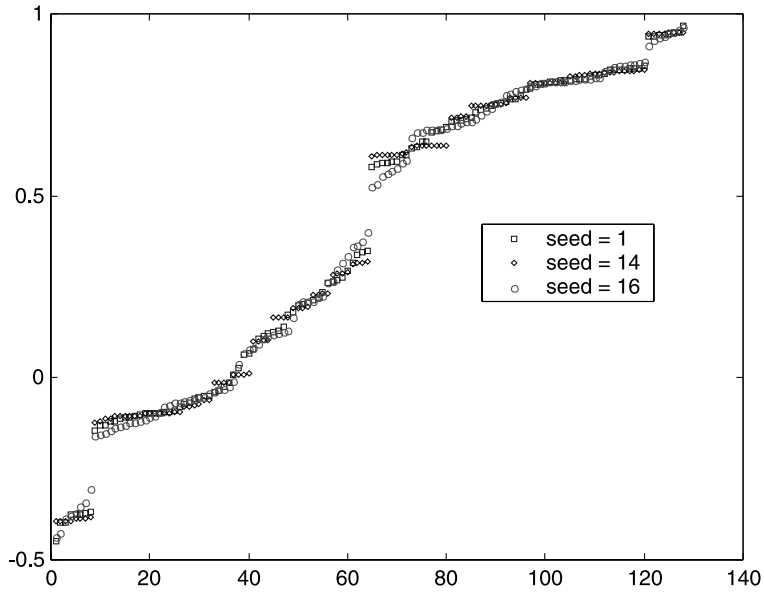


Fig. 6. Sorted possible values of the solution of the system for different initial conditions.

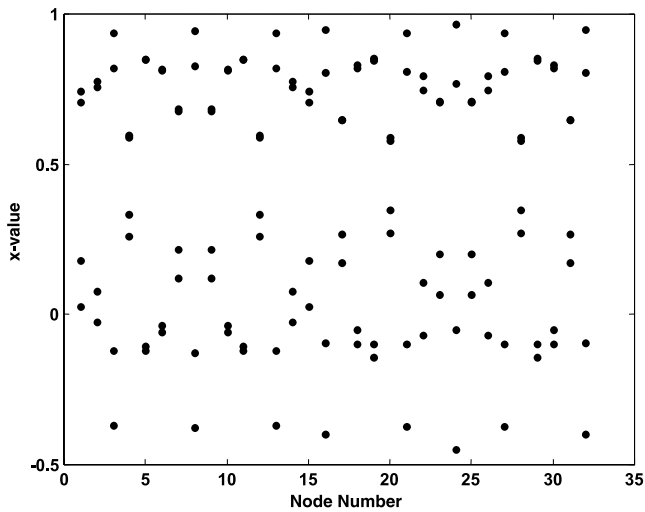


Fig. 7. Projections of the values of the oscillators for every node using random initial conditions generated with a seed of 5.

is the same as that for node 9, similarly, node 6 is the same as node 10, and so on.

The symmetry in the response of the system indicated by Fig. 7 is further explored in Fig. 8. Here  $p$  corresponds to the state of the dynamical system (2) after 2,000,000 iterations. The solid large dot again indicates node 8 and the solid small dot indicates node 24, the node numbers increasing counterclockwise. Symmetry with respect to an axis passing through nodes 8 and 24 is now clearly seen.

Our numerical exploration included 20 different random initial conditions (seeds with values  $s$  ranging from 1 to 20) for the parameter values  $b = 0.2$  and  $\alpha = 1.9$ ; in each case a 4-period global response asymptotically emerged. All except three of the 4-period, non-symmetric, solutions were found to be different, indicating that numerous different 4-period solutions exist. We are thus led to conclude from the above numerical results that for the ring structure (and parameter values) used in this section it is possible for the global behavior of the oscillator-ring to exhibit a *large variety of different* (asymptotically stable) periodic solutions depending on the choice of initial conditions, that numerous 4-period attractors therefore exist, each leading to a different, stable, 4-period orbit.

The variation of the global response as the parameter  $b$  is altered from 0 to 0.5 is shown in Fig. 9 when the initial conditions are generated using a seed value  $s = 1$ . The largest three LCEs are shown for each value of  $b$ . The system, in each case, is allowed to evolve for 5,020,000 iterations, and the LCEs are

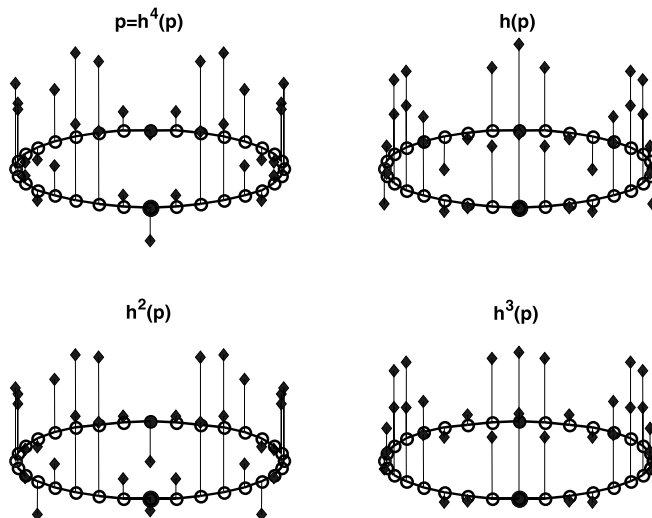


Fig. 8. Periodic solutions using a seed of 5.

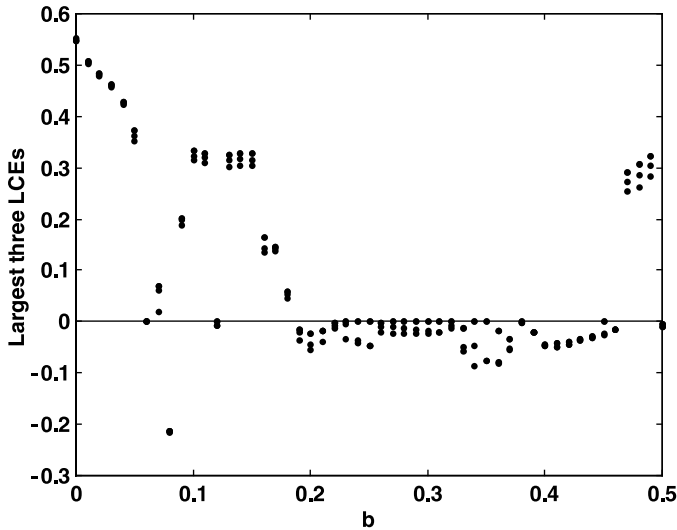


Fig. 9. The largest three LCEs of the system for different values of  $b$ ,  $\alpha = 1.9$ , with a seed of  $s = 1$ .

computed using the subsequent 50,000 iterations. One observes that a chaotic response is more likely to result from the coupled ring when the interconnection strength is either very high or very low (when  $b < 0.18$  and  $b$  close to 0.5). It should be pointed out though that in several cases the largest LCE turns out to be perilously close to zero, making the distinction between chaotic and non-chaotic responses difficult to differentiate, based solely on the LCE values.

To illustrate the complexity of the responses, we show in Fig. 10 the responses obtained when  $b = 1/3$  and  $\alpha = 1.9$ . A variety of solutions are now obtained for different initial conditions (seed values). We illustrate three different types here: an 8-period solution, a sample of the 4-period solutions (each different from one another), and a sample of the chaotic solutions. These are illustrated in Fig. 10(a)–(c). While the largest LCEs for the 4-period solutions and the 8-period solution are discernably negative, the largest LCEs for the chaotic solution is 0.0000192, a value so close to zero, that one has to carefully study the responses to ascertain the nature of the solution.

For later comparison, we show in Fig. 11 a plot similar to Fig. 9 where the largest three LCEs are plotted versus  $b$ , this time for the homogeneous ring with  $\alpha = 1.5$ . Where  $b$  to be zero, and the oscillators uncoupled, each would exhibit a chaotic response with a positive Lyapunov characteristic exponent of 0.241. The LCEs are again computed (with a seed of unity) using 50,000 iterations at the end of 5,020,000 iterations. It should be noted that for several values of  $b$  where the largest LCE appears close to zero, the response could be chaotic.

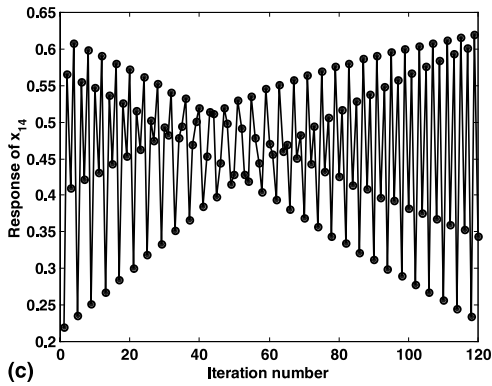
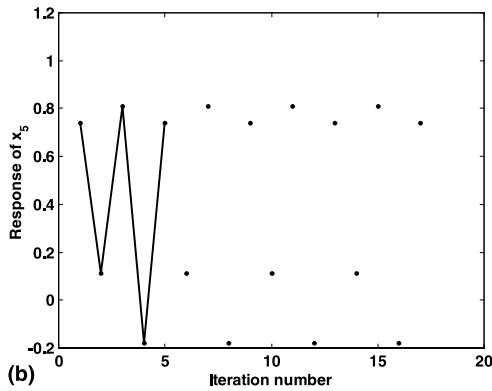
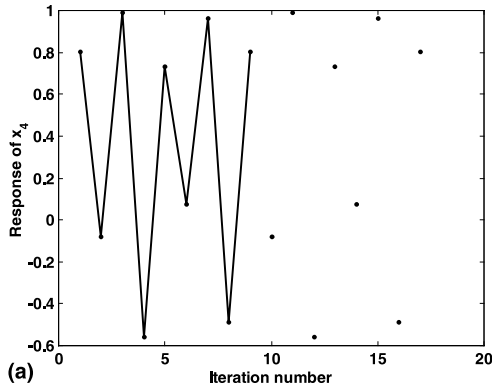


Fig. 10. Structurally different solutions for different initial conditions,  $b = 1/3$ ,  $\alpha = 1.9$ : (a) response of node  $x_4$  showing an 8-period solution; (b) response of node  $x_5$  showing an 4-period solution; (c) response of node  $x_{14}$  showing a chaotic solution.

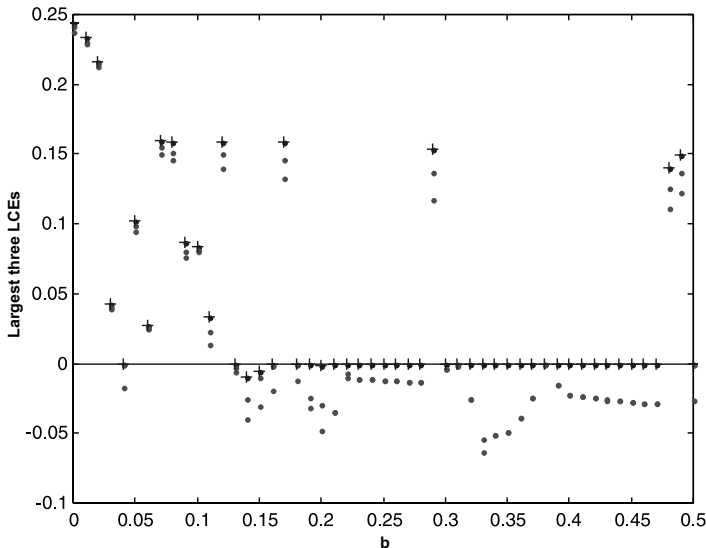


Fig. 11. The largest three LCEs of the system for different values of  $b$ ,  $\alpha = 1.5$  using a seed of  $s = 1$ .

The wide range in the types of responses of rings of identical oscillators even includes traveling waves. Fig. 12 shows a traveling wave which occurs for the parameter values of  $b = 0.4$  and  $\alpha = 1.9$ . To generate the wave, the initial conditions with a seed of  $s = 1$  were used. The system settled into a periodic solution, and the value of  $n$  shown in the figure corresponds to the 2,000,000th iteration. As before, the small (solid) dot indicates node number 24, and the large (solid) dot indicates node number 8.

### 3.2. A ring of non-identical oscillators

In this section we present numerical results showing the types of global behavior that could accrue when the oscillators are *not* identical. We again consider a ring of  $n = 32$  oscillators, where  $3/4$  of the ring (the first 28 oscillators) have  $\alpha = 1.9$  associated with them, and the remaining  $1/4$  (8 oscillators) have  $\alpha = 1.5$  (see Fig. 13). The connection parameter values are taken to be  $a = 0.6$  and  $b = 0.2$ .

Fig. 14 shows four initial conditions together with the corresponding approximations of the largest three LCEs of the system as a function of iteration number. Here, the computation of the LCEs is initiated after the first 2,000,000 iterations, and the LCEs are estimated using the next 50,000 iterations. Two initial conditions for the dynamical system (described by Eq. (2)) are generated

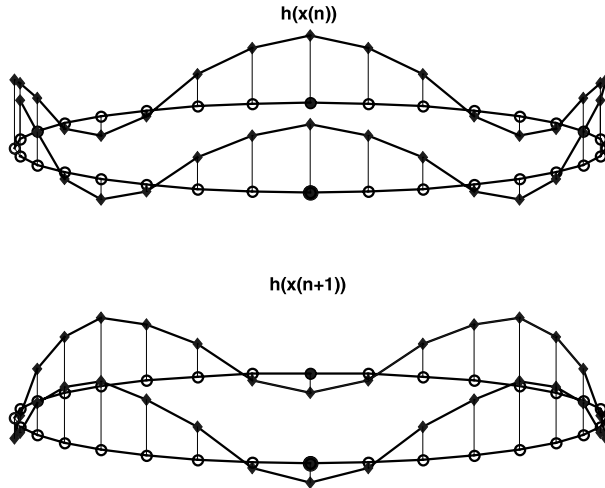


Fig. 12. Traveling wave using parameter values  $b = 0.4$ ,  $\alpha = 1.9$  and seed  $s = 1$ .

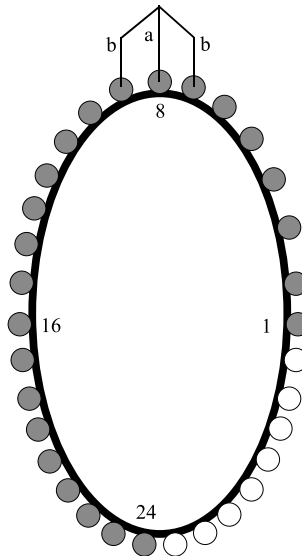


Fig. 13. Ring with  $n = 32$  oscillators. Solid dots represent oscillators with  $\alpha = 1.9$ ; open dots represent oscillators with  $\alpha = 1.5$ .

using a sinusoid of the general form  $x_j(0) = \mu \sin(v\pi(j - 1)/(n - 1))$ . The top set of initial conditions (Fig. 14(a)) use  $\mu = 0.1$ , and the next set (Fig. 14(b)) uses  $\mu = 0.85$ ; in both cases  $v = 5$ . For the case of  $\mu = 0.1$ , the system has only

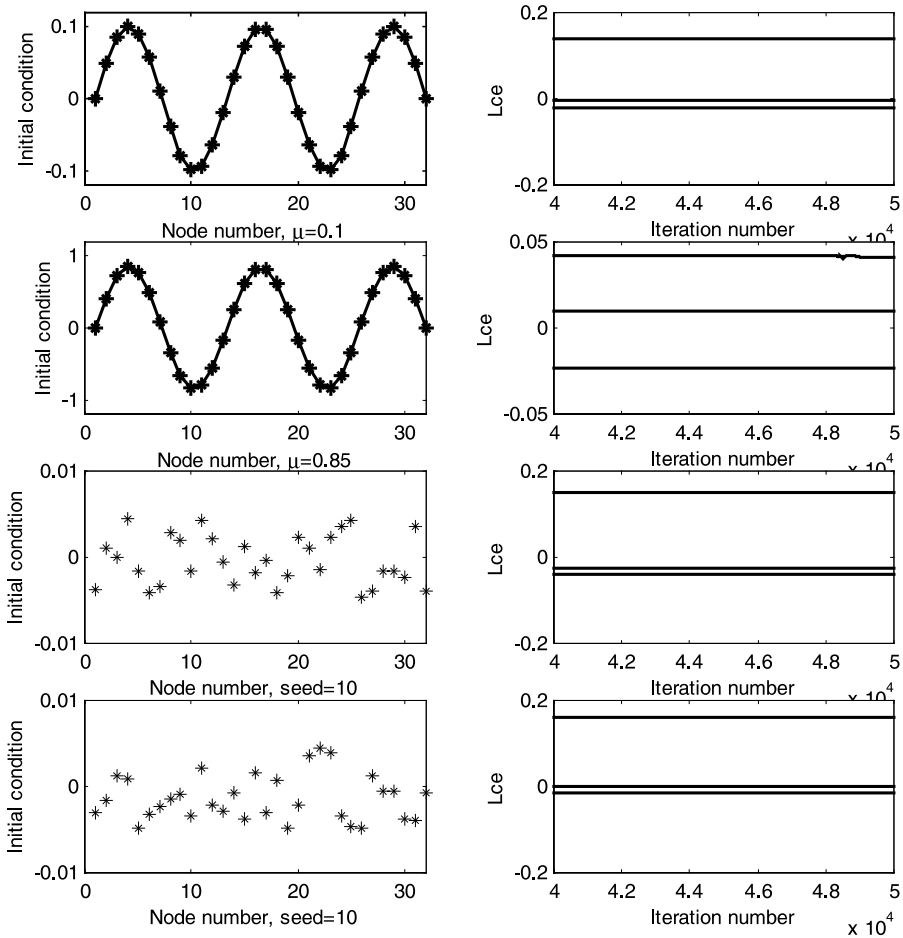


Fig. 14. Largest three LCEs of the system and corresponding initial conditions.

one positive LCE, while for the case of  $\mu = 0.85$ , the system has two positive LCEs. Fig. 14(c) and (d) show the LCEs determined when the initial conditions are obtained by using a random seed  $s = 10$ , as before. The first 32 random numbers generated are used as the initial conditions for Fig. 14(c), the next 32 for Fig. 14(d). As seen from the figure, the largest three LCEs in each case are different. The fact that the number of positive LCEs can vary with the initial conditions, shows that the system can end up with very different attractors depending on the initial conditions that are used.

Fig. 15 shows the projection of the solutions at each node (identifying the possible response ‘Location’ of the oscillator) starting from the iteration

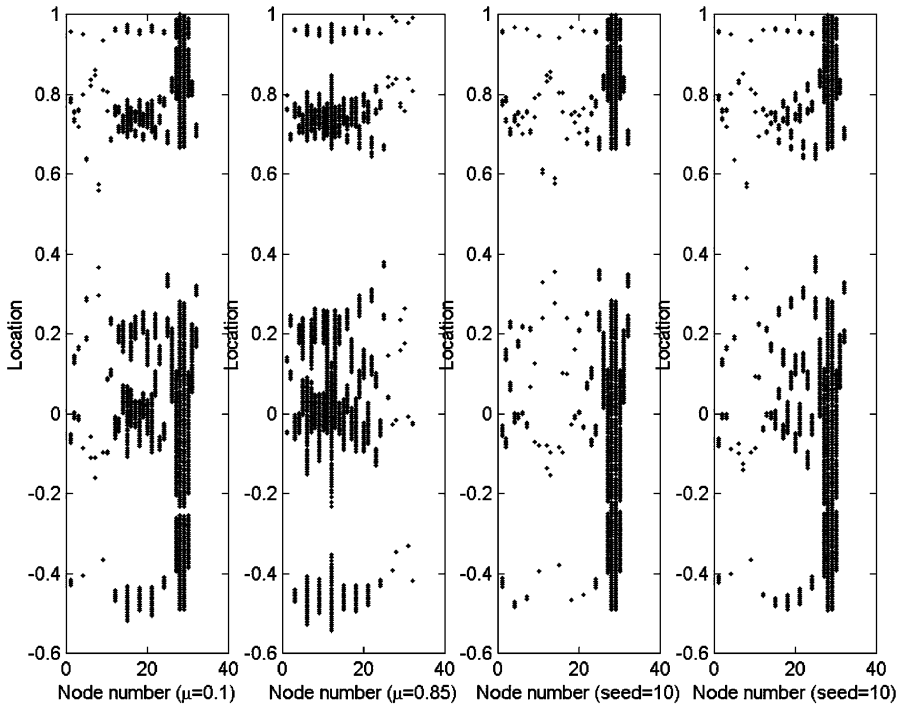


Fig. 15. Projection of the solutions at each node for the three cases. The left most plot corresponds to the initial condition using  $\mu = 0.1$ , the next to the case using  $\mu = 0.85$ , and the right most two correspond to the case when different random initial conditions were used.

number 2,000,000 up to iteration number 2,002,000 for the four cases. We record these projections on the axis labeled 'Locations'. The figure gives an idea about the 'shape' of the attractors, and it clearly suggests that the attractors are different.

The complexity of the global response of the non-homogeneous ring as the connection strength  $b$  is varied is shown in Fig. 16. Here 50,000 iterations are used to compute the largest three LCEs at the end of 5,020,000 iterations. Comparing this figure with Figs. 9 and 11, we observe that chaotic responses are generated for both small and large values of  $b$ . Most of the values of  $b$  for which the LCEs are close to zero can be found in the band  $0.28 < b < 0.36$ . For  $b = 1/3$ , our computations for this inhomogeneous ring, starting from 20 different seeds, all yielded only 4-period solutions. However, several different 4-period solutions exist, corresponding to different values of the seed,  $s$  (recall the presence of chaotic solutions for the homogeneous ring ( $\alpha = 1.9$ ) with the same  $b$  value, see Fig. 10).

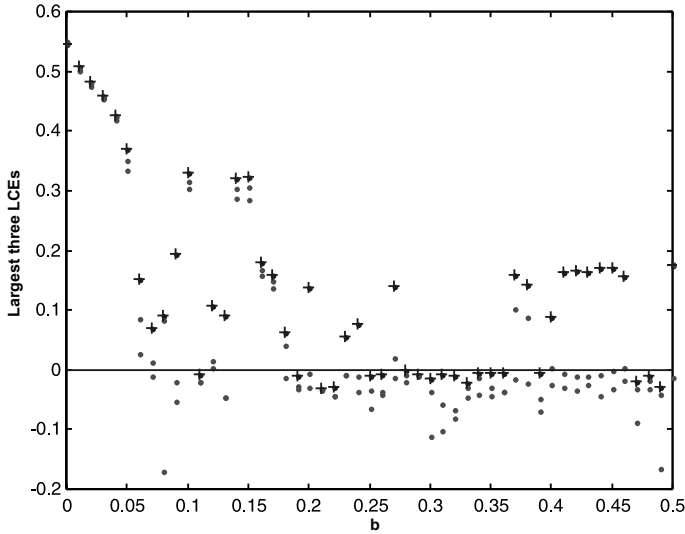


Fig. 16. The largest three LCEs of the system for different values of  $b$ , of the non-homogeneous ring.

#### 4. Model of two coupled rings of oscillators

Considering each ring as a ‘compartment’, in this section, we explore what the global response of a system comprising two such connected compartments might be. We consider two oscillator-rings with  $n$  oscillators each, say ring  $X$  and ring  $Y$ ; each ring has the structure presented in Section 2, see Fig. 17. In general, the two rings may not be identical. The two rings  $X$  and  $Y$  can be coupled leading to a dynamical system of the following form:

$$\begin{bmatrix} x(i+1) \\ y(i+1) \end{bmatrix} = \begin{bmatrix} \tilde{A} & \tilde{C}_{xy} \\ \tilde{C}_{yx} & \tilde{B} \end{bmatrix} \begin{bmatrix} \tilde{f}(x(i), \alpha_x) \\ \tilde{f}(y(i), \alpha_y) \end{bmatrix}. \quad (6)$$

In Eq. (6), the response at the  $i+1$  step of the oscillators in the  $X$  ring is given by the  $n$ -vector  $x(i+1)$ , and similarly, the  $n$ -vector  $y(i+1)$  is the response of the oscillators in the  $Y$  ring. The values of  $\tilde{A}$ ,  $\tilde{B}$ , and the coupling matrices  $\tilde{C}_{xy}$  and  $\tilde{C}_{yx}$  are obtained after normalizing the row sum of each row of the matrix  $H$  to unity, where  $H$  is given by

$$H = \begin{bmatrix} A & C_{xy} \\ C_{yx} & B \end{bmatrix}, \quad (7)$$



conditions for each of the two rings was found to yield a chaotic response of the connected system. These results are shown in Figs. 18 and 19(a) where the LCEs and the response  $x_{12}(t)$  of the connected system are computed. Fig. 18 shows the LCEs when the same initial conditions (seed  $s = 1$ ) are used to generate the 32-element initial vector for each ring; the vector of initial conditions for the second ring is then rotated relative to that for the first through 3 nodes.

Fig. 19(a) shows the chaotic response when the left-hand ring has initial conditions corresponding to  $s = 1$  and the right-hand ring has initial conditions obtained by using  $s = 10$ . The response of  $x_{12}(t)$  is also shown in both figures, illustrating the chaotic behavior. We have noted earlier that with each of these initial conditions, the responses of each of the individual oscillator-ring compartments yield 4-period solutions asymptotically (see Table 1). Upon connecting the two compartments ( $C_{xy} = C_{yx} = 0.2$ ), the response after 5,070,000 iterations of the system is chaotic. If after the chaotic response has been generated, the connection is broken ( $C_{xy} = C_{yx} = 0.0$ ), the responses of the individual rings revert back to a 4-period solution. Finally, if the system is reconnected ( $C_{xy} = C_{yx} = 0.2$ ) after the 4-period solutions are reached, the response of the system is again chaotic after 5,070,000 iterations. We have thus illustrated that while each separate compartment exhibits periodic response, the response of the system when the two compartments are connected becomes

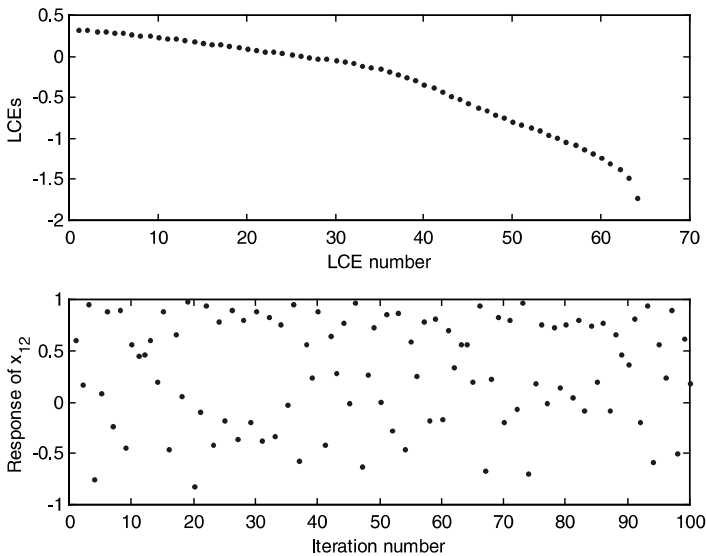


Fig. 18. LCEs and response of  $x_{12}(t)$  when using random initial conditions with  $s = 1$  for ring  $X$  and same initial conditions, but shifted by three elements, for ring  $Y$ .

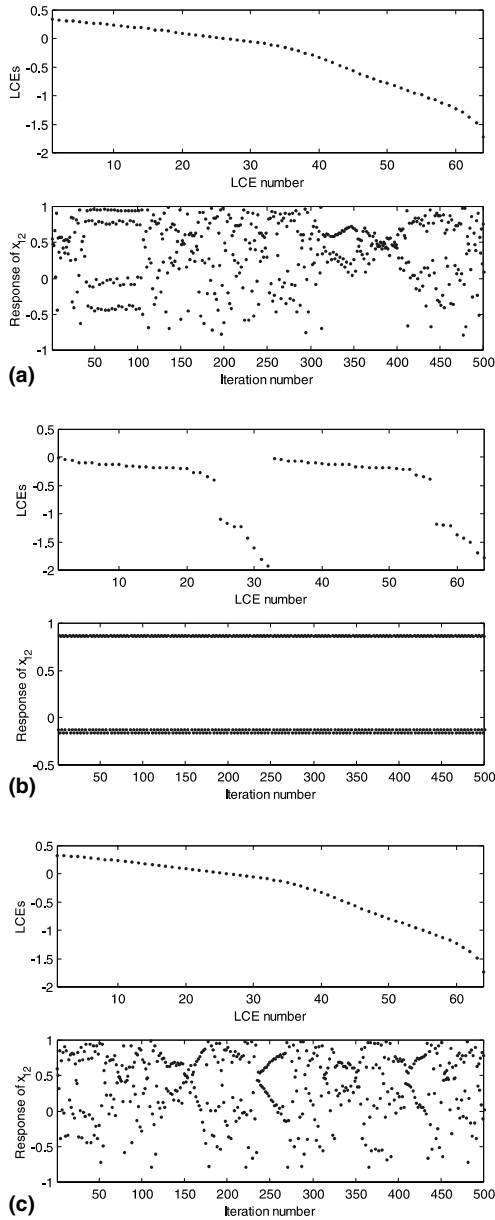


Fig. 19. (a) LCEs and response of  $x_{12}(t)$  for connected rings when using random initial conditions with  $s = 1$  for ring  $X$  and  $s = 10$  for ring  $Y$ . (b) LCEs and response of  $x_{12}(t)$  after disconnecting the rings. (c) LCEs and response of  $x_{12}(t)$  after reconnecting the rings.

chaotic; furthermore with the severance of this connection the response of each ring reverts to periodic behavior. This is indeed reminiscent to the reduction in brain activity when the corpus collosum is severed between the right half and the left half of the brain. Fig. 19 shows the evolution of the dynamics of the system, first with connection ( $C_{xy} = C_{yx} = 0.2$ , in Fig. 19(a)), followed by a disconnection ( $C_{xy} = C_{yx} = 0$ , in Fig. 19(b)), between the first node of each ring, and at last, a reconnection of the two rings ( $C_{xy} = C_{yx} = 0.2$ , in Fig. 19(c)).

We next consider the variation of the global response of the interconnected compartments as the strength of the interconnection is varied. We look at two rings with 32 oscillators each with the first node of one oscillator-ring connected to the first node of the second. The coupling matrices are such that  $C_{xy} = C_{yx}$ , and  $C_{xy}(1, 1) = c$ , with all other entries equal to zero. The coupling strength parameter  $c$  was ranged from  $c = 0$  to  $c = 1.5$ . Both rings are identical, with  $\alpha = 1.9$ ,  $a = 0.6$ , and  $b = 0.2$ .

Fig. 20 shows a plot of the largest three LCEs versus the coupling strength  $c$ . For each value of  $c$ , the LCEs were computed for 50,000 iterations (after skipping the first 5,020,000 points of the trajectory). For a given  $c$ , the largest three LCEs recorded on the plot corresponds to the LCEs at the 50,000th iteration. The random initial condition for one compartment was generated by using a seed  $s = 1$ ; the initial condition for the other by using a seed  $s = 10$ .

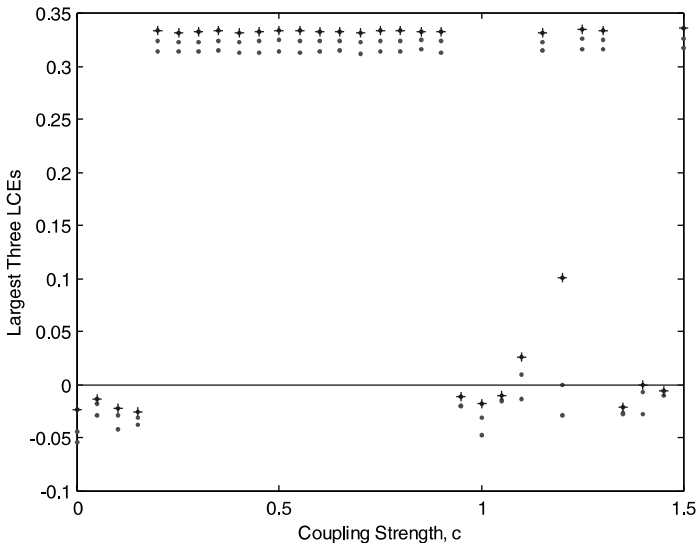


Fig. 20. Largest three LCEs versus the coupling strength  $c$ . The oscillator-rings are identical with  $\alpha = 1.9$ ,  $a = 0.6$ , and  $b = 0.2$ .

The figure shows that, in general, as the coupling strength increases until  $c = 0.9$ , the response of the connected compartments is more likely to be chaotic. After  $c = 0.9$ , the type of response of the system seems less predictable; there is mixture of periodic and chaotic responses.

#### 4.2. Effects of coupling location on inhomogeneous oscillator-ring compartments

For the cases considered in this part, basically, two copies of the ring presented in Fig. 13 were coupled, that is,  $A = B$ , with  $a = 0.6$  and  $b = 0.2$ , and  $\alpha_x = \alpha_y$ , with the same distribution of the values of  $\alpha$  as in Fig. 13. Random initial conditions were generated, and the same set of random initial conditions were used for each of the four coupling cases (in MATLAB code, the initial conditions,  $x_i$ , were generated using the commands: `rand('seed',10)`,  $x_i = (\text{rand}(64, 1) - 0.5)/100$ . The first 32 random numbers were assigned as initial values to the first compartment, the next 32 to the second compartment. For the coupling, four oscillators of the ring  $X$  were connected to four oscillators of ring  $Y$ . In each case, the first 2,000,000 points of trajectory were computed, then for the next 50,000 iterations the LCEs were computed. Next we present the numerical results for four different cases of the coupling considered. For each coupling case considered, we show four plots that help us characterize the response. The first subplot shows the trajectory of the oscillators  $x_{12}$  and  $x_{27}$ , (the 50 iterations shown correspond to the iterations from 2,049,900 to 2,049,950). The next subplot presents the largest 10 LCEs of the system (the values shown correspond to the LCEs at the 50,000th iteration of computing the LCEs, which corresponds to the 2,050,000th iteration of the trajectory). The remaining subplots show the delayed responses of oscillators  $x_{12}$  and  $x_{27}$  (50 points are plotted in each figure and they correspond to the response of the system for iteration values close to 2,049,900). Each ring can be divided into four quadrants, the first 8 oscillators would lie in the first quadrant, the next 8 oscillators in the second quadrant and so on. With this categorization of rings into quadrants, we consider the following different connections cases.

##### **Case 1.** *Connecting oscillators from the fourth quadrant of ring $X$ to oscillators from the fourth quadrant of ring $Y$ .*

As shown in Fig. 21(a), the oscillators with  $\alpha = 1.5$  of ring  $X$  are connected to oscillators with  $\alpha = 1.5$  of ring  $Y$ . Node  $x_{27}$  is connected with  $y_{27}$ ,  $x_{28}$  with  $y_{28}$ ,  $x_{29}$  with  $y_{29}$ , and  $x_{30}$  with  $y_{30}$ . The connections in term of the coupling matrices are such that  $C_{xy} = C_{yx}$ , and  $C_{xy}(27, 27) = C_{xy}(28, 28) = C_{xy}(29, 29) = C_{xy}(30, 30) = c = 0.65$ , with all other entries equal to zero.

The results from the numerical computations are shown in Fig. 21(b). The responses of the oscillators  $x_{12}$  and  $x_{27}$  shown in the first subplot suggest the system has a periodic response (note: the response of the other oscillators not

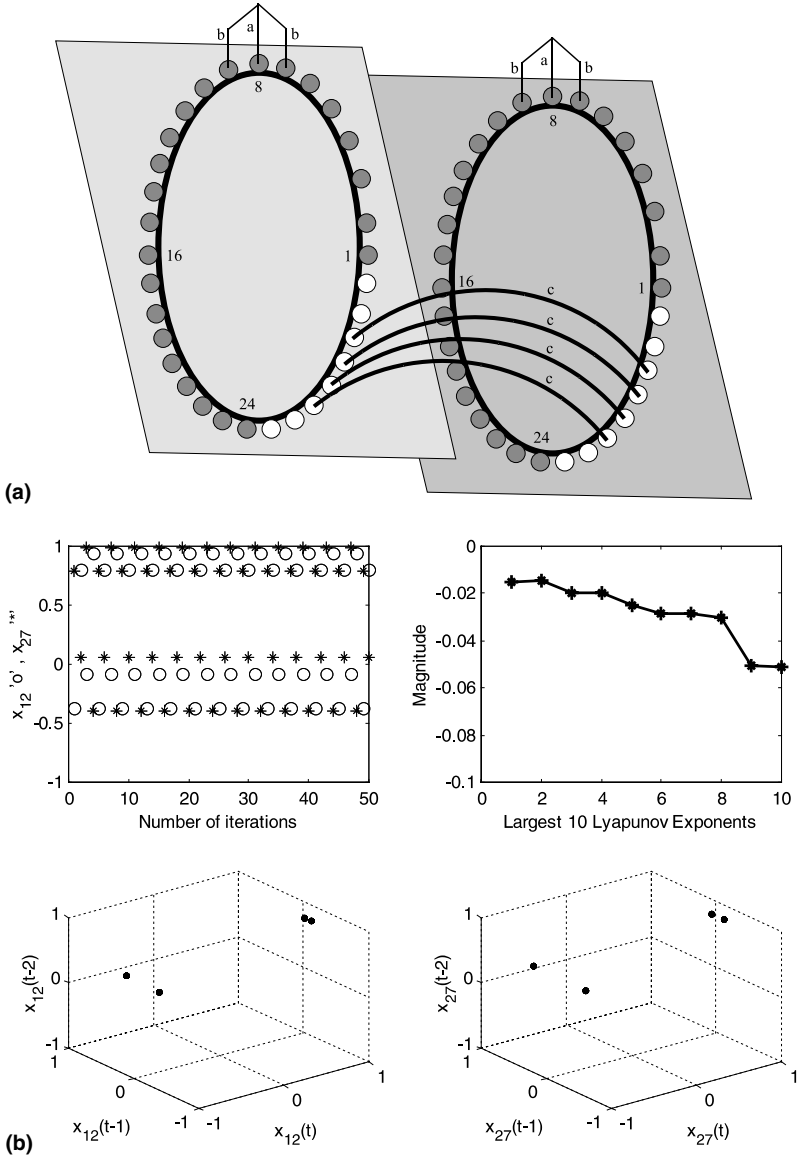


Fig. 21. (a) Coupling for Case 1, open circle have  $\alpha = 1.5$  and closed circles have  $\alpha = 1.9$ . (b) Numerical results for Case 1.

shown here, also suggest a periodic response). Note that all the LCEs shown in the next subplot are negative, also suggesting that the response of the system is periodic. The plots of the delayed responses of oscillators  $x_{12}$  and  $x_{27}$  shown in

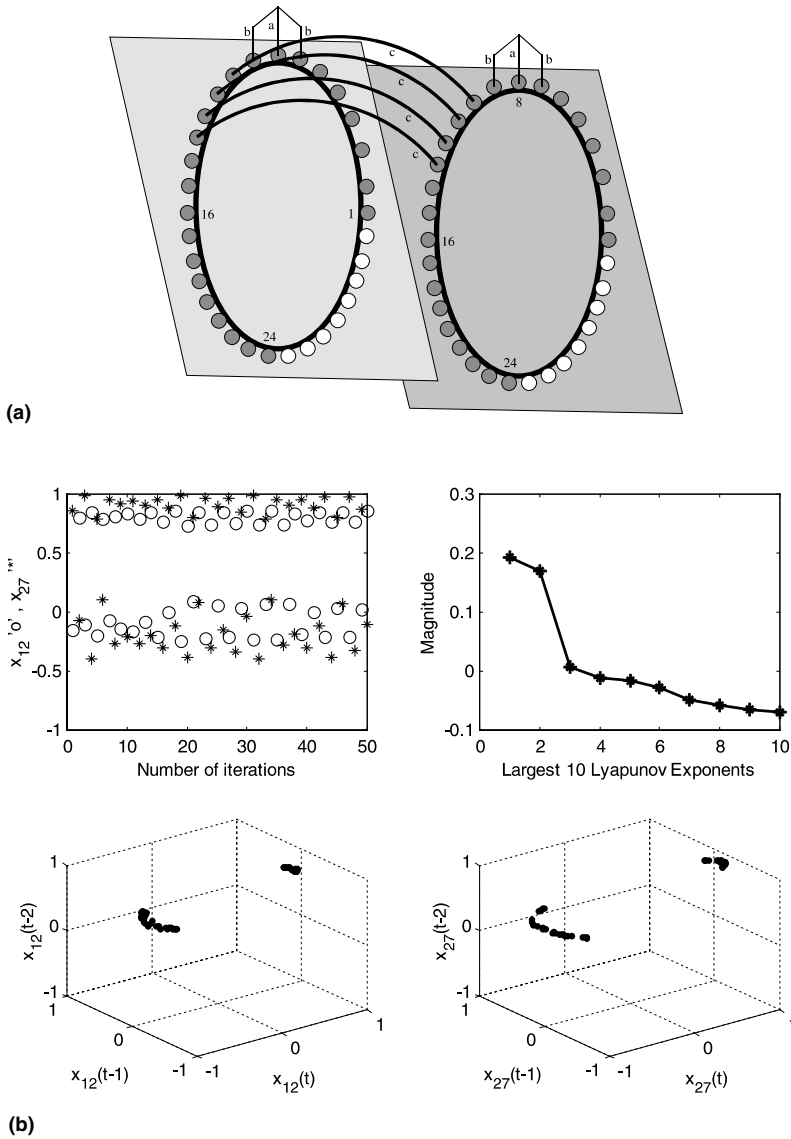


Fig. 22. (a) Coupling for Case 2, open circle have  $\alpha = 1.5$  and closed circles have  $\alpha = 1.9$ . (b) Numerical results for Case 2.

the last two subplots, suggest once again that the system has a periodic response under the coupling used in this case. Though each of the separate inhomogeneous compartments exhibits a chaotic response, the coupled response is periodic.

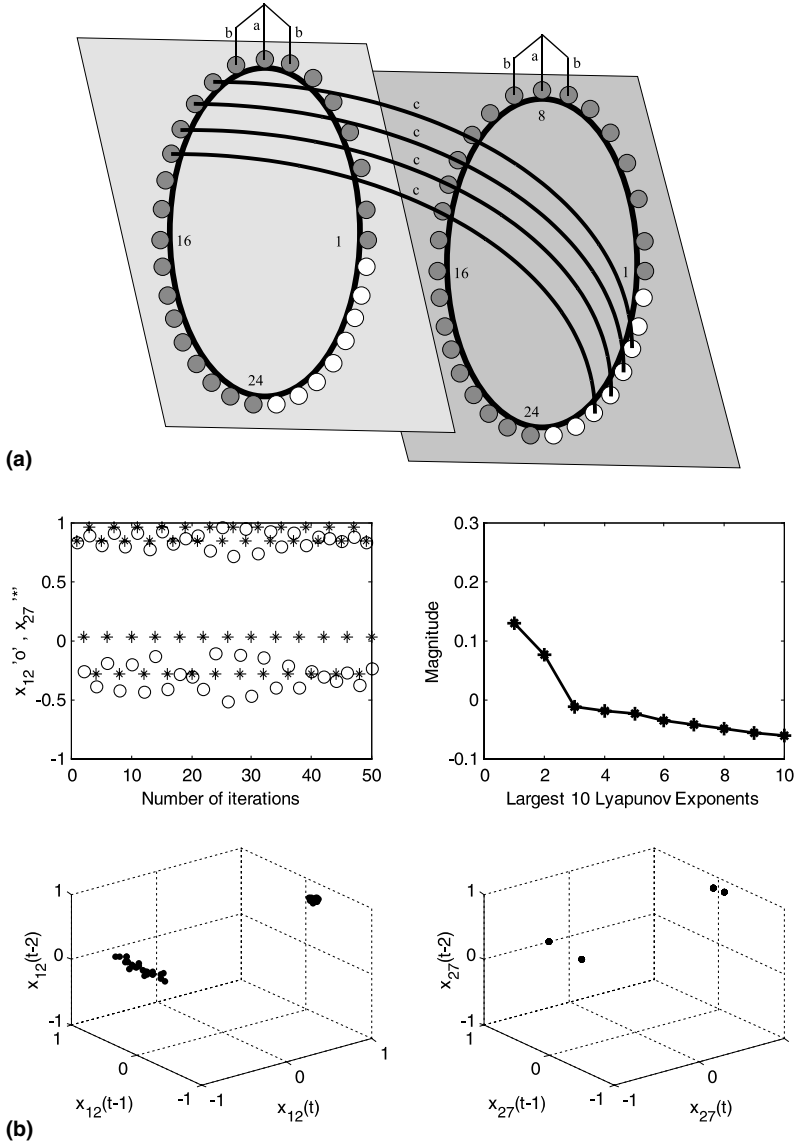


Fig. 23. (a) Coupling for Case 3, open circle have  $\alpha = 1.5$  and closed circles have  $\alpha = 1.9$ . (b) Numerical results for Case 3.

**Case 2.** Connecting oscillators from the second quadrant of ring  $X$  to oscillators from the second quadrant of ring  $Y$ .

Here oscillators with  $\alpha = 1.9$  of ring  $X$  are connected to oscillators with  $\alpha = 1.9$  of ring  $Y$  as shown in Fig. 22(a). The coupling matrices are such that

$C_{xy} = C_{yx}$ , and  $C_{xy}(10, 10) = C_{xy}(11, 11) = C_{xy}(12, 12) = C_{xy}(13, 13) = c = 0.65$ , with all other entries equal to zero.

The results from the numerical computations are shown in Fig. 22(b). The response of the oscillators  $x_{12}$  and  $x_{27}$  shown in the first subplot, suggests the system is chaotic (note: the response of the other oscillators not shown here, also suggests a chaotic response). The fact that we have some (three) positive LCEs, as shown in the next subplot, suggests that the system is chaotic. The remaining subplots also indicate chaotic behavior.

**Case 3.** *Connecting oscillators from the second quadrant of ring X to oscillators from the fourth quadrant of ring Y.*

This case is shown in Fig. 23(a), where the oscillators with  $\alpha = 1.9$  of ring X are connected to oscillators with  $\alpha = 1.5$  of ring Y. The coupling matrices are such that  $C_{xy} = C_{yx}$ , and  $C_{xy}(10, 30) = C_{xy}(11, 29) = C_{xy}(12, 28) = C_{xy}(13, 27) = c = 0.65$ , with all other entries equal to zero.

The results from the numerical computations are shown in Fig. 23(b). The response of  $x_{12}$ , shown in the first subplot, suggests that the system is chaotic. The two largest LCEs shown in the next subplot, are positive suggesting a chaotic response. The plot displaying the delayed values of  $x_{12}$ , shown in the next subplot confirms this.

**Case 4.** *Connecting oscillators from the first quadrant of ring X to oscillators from the first quadrant of ring Y.*

Here oscillators with  $\alpha = 1.9$  of ring X are connected to oscillators with  $\alpha = 1.9$  of ring Y, as shown in Fig. 24(a). The connections in term of the coupling matrices are such that  $C_{xy} = C_{yx}$ , and  $C_{xy}(1, 1) = C_{xy}(2, 2) = C_{xy}(3, 3) = C_{xy}(4, 4) = c = 0.65$ , with all other entries equal to zero.

The results from the numerical computations are shown in Fig. 24(b). The response of both  $x_{12}$  and  $x_{27}$ , shown in the first subplot, suggest that the system is chaotic, but in particular  $x_{27}$ . The five largest LCEs are positive suggesting a chaotic response, as shown in the next subplot. The remaining subplots show the delayed responses of oscillators  $x_{12}$  and  $x_{27}$ . The plot of the delayed values of  $x_{27}$  suggests that the system is chaotic.

The number of positive LCEs of the system changes as we change the type of connection. This fact suggests that the structure of the invariant sets for each of these cases is different. These differences can also be observed in the responses that have been provided.

## 5. Conclusions and comments

In this paper we have explored the dynamical behavior of coupled nonlinear systems. We use as our basic nonlinear system, or elemental unit, a chaotic

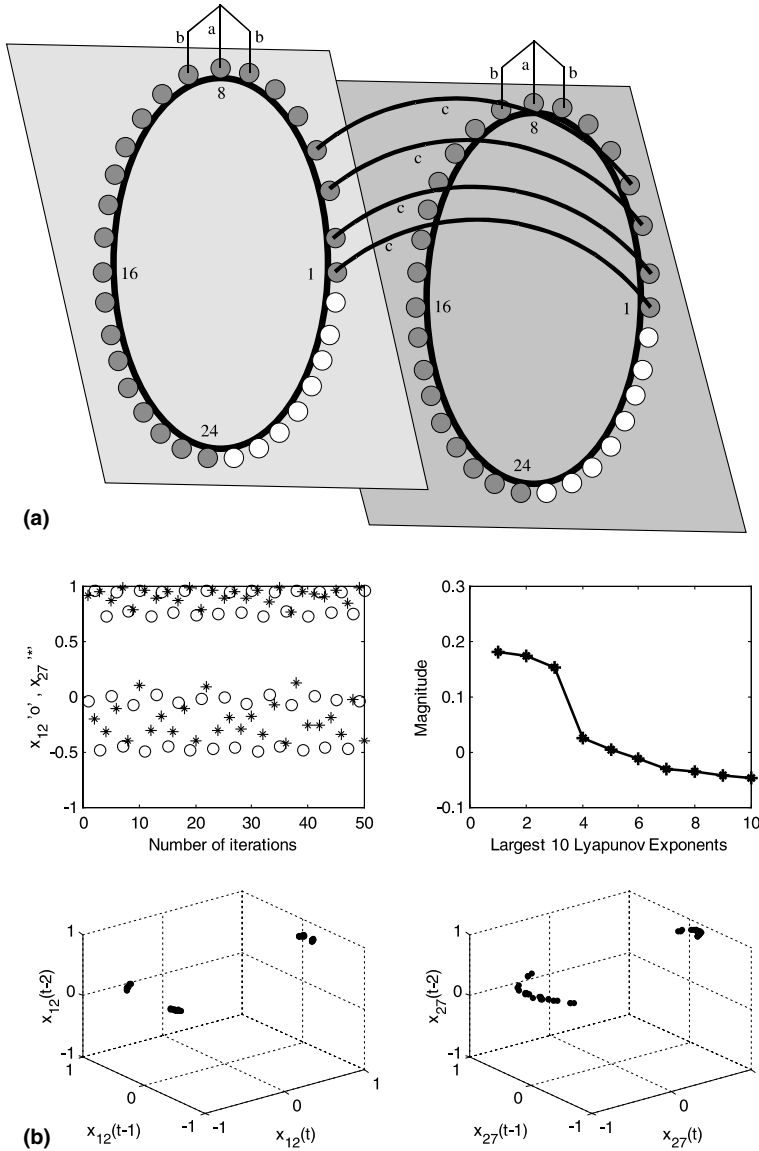


Fig. 24. (a) Coupling for Case 4, open circle have  $\alpha = 1.5$  and closed circles have  $\alpha = 1.9$ . (b) Numerical results for Case 4.

system described by a simple nonlinear map. We connect these units into a ring and explore the dynamics of such rings. We begin by making some specific conclusions that this study indicates and then provide some general comments.

1. We find that though each unit may be chaotic, the coupled oscillator-ring may exhibit periodic global behavior asymptotically. This behavior usually emerges rather abruptly after a considerable number of iterations pointing to a transient chaos phenomenon. In the example considered we show that a multiplicity of different four periodic solutions can be exhibited by the homogeneous oscillator-ring, each solution being an attractor for a different initial condition. The variation in the global behavior of an oscillator-ring with changes in the coupling parameters is also explored; both very weak ( $b \approx 0$ ) and very strong ( $b \approx 0.5$ ) coupling seem to engender chaotic global responses.
2. The global behavior of non-homogeneous rings is also explored and its complexity is exhibited, as the coupling parameter  $b$  is altered.
3. The behavior of identical coupled oscillator-rings is next explored, and it is shown that even when each ring (or compartment) exhibits periodic behavior, the coupled system may behave chaotically. Cutting the connection between the two compartments can restore periodic behavior in each of them. Reconnection could yield again chaotic behavior.
4. Lastly we consider the coupled behavior of non-homogeneous rings and show the sensitivity of the global response of the combined system to the location of the coupling.

Our computer experiments show the enormous complexity of coupled dynamical systems. At present we have no theories which predict the types of global behaviors observed. We hope that our numerical results will incite theoreticians to explore the possible explanations for several of the types of responses which we have computationally observed here. For example, with respect to the first point mentioned above, several theoretical questions seem relevant: Why does transition to periodic behavior occur so abruptly? Can it be explained as a boundary crisis? How many 4-period solutions are there for the specific system parameters chosen? Why does the system settle to a 4-period response?

The third point reinforces our belief that understanding the behavior of nonlinear systems depends heavily on the level of granularity at which one ‘observes’ the system. At the level of each isolated elemental unit in our case, the system appears chaotic; at the level of the oscillator-ring, several example systems shown in this paper behave periodically; at the level of two coupled oscillator-rings, the behavior could again be chaotic. The behaviors at the various levels of granularity are strongly and sensitively dependent on the parameters that describe the level and extent of interconnection.

If one oscillator-ring is thought of as a metaphor for the left hemisphere of the human brain, the other for the right, and each elemental unit thought of as a neuron, our model (though a drastic caricature) shows that periodic responses (some sort of learning, or memory) show up in each hemisphere after a considerable number of iterations, that they occur abruptly, and that a con-

nection between the two hemispheres could lead to chaotic activity, depending on the extent and level of connection between the two hemispheres. One is reminded of the incidence of epilepsy and its possible treatment through the cutting of the connection between the two brain hemispheres. This restores periodic behavior in each ring-hemisphere in our model.

If one is to begin to understand the dynamical behavior of complex, large-scale coupled systems like the human brain, one would need to start with developing a theoretical understanding of the types of interconnected nonlinear dynamical systems (and responses) explored computationally in this paper. At present we are ignorant of how to predict global patterns of behavior in large-scale interconnected nonlinear systems, based on the knowledge of the behavior of the individual, elemental, interconnected units and their local interactions. We hope that this challenge will be taken up by the nonlinear dynamicists.

Lastly, we point out that much more computational experimentation is needed to exhibit and understand the behavior of complex coupled nonlinear systems. In that sense, this study represented merely ‘a small tip of the iceberg’.

## References

- [1] Turing, The chemical basis of morphogenesis, *Philos. Trans. R. Soc. Lond. [Biol]* 237 (1952) 37–72.
- [2] D.A. Linkens, I. Taylor, H.L. Duthie, Mathematical modeling of the colorectal myoelectrical activity in humans, *IEEE Trans. Biomed. Eng.* 23 (1976) 101–110.
- [3] I. Morishita, A. Yajima, Analysis and simulation of networks of mutually inhibiting neurons, *Kybernetik* 11 (1972) 154–165.
- [4] S.J. Bay, H. Hemami, Modeling of neural pattern generator with coupled nonlinear oscillators, *IEEE Trans. Biomed. Eng.* 34 (1987) 297–306.
- [5] S. Grillner, P. Wallen, Central pattern generation for locomotion with special reference to vertebrates, *Annual Rev. Neurosci.* 8 (1985) 233–261.
- [6] O.W. Freisen, G.S. Stent, Neural circuits for generating rhythmic movements, *Annual Rev. Biophys. Bioeng.* 7 (1978) 37–61.
- [7] A. Atiya, P. Baldi, Oscillations and synchronizations in neural networks: an exploration of the labelling hypothesis, *Int. J. Neural Syst.* 1 (1989) 103–124.
- [8] G.B. Ermentrout, The behavior of rings of coupled oscillators, *J. Math. Biol.* 23 (1985) 55–74.
- [9] N. Nishiyama, Experimental observation of dynamical behaviors of 4, 5, and 6 oscillators in rings and nine oscillators in branched network, *Phys. D* 80 (1995) 181–185.
- [10] M.A. Matias, Observation of fast rotating wave in rings of coupled chaotic oscillators, *Phys. Rev. Lett.* 78 (1997) 219–222.
- [11] J. Collins, I. Stewart, A group-theoretic approach to rings of coupled biological oscillators, *Biol. Cybern.* 71 (1994) 95–103.
- [12] K. Kaneko, *Theory and Applications of Coupled Map Lattices*, Wiley, Chichester, 1993.
- [13] A. Kouda, S. Mori, Analysis of a ring of mutually coupled Van der Pol oscillators with coupling delays, *IEEE Trans. Circuit Syst.* 28 (1981) 247–253.
- [14] J. Grasman, M.J.W. Jensen, Mutually synchronized relaxation oscillators as prototypes of oscillating systems in Biology, *J. Math. Biol.* 7 (1979) 171–197.

- [15] E.F. Udawadia, N. Raju, Dynamics of coupled nonlinear maps and its application to ecological modeling, *Appl. Math. Comput.* 82 (2&3) (1997) 137–179.
- [16] M.A. Mathias, J. Guemez, V. Perez-Munuzuri, I. Marino, M. Lorenzo, V. Perez-Villa, Size instabilities in rings of chaotic synchronized systems, *Europhys. Lett.* 37 (1997) 379–384.
- [17] H. von Bremen, On the computation of Lyapunov characteristic exponents, Ph.D. Dissertation, University of Southern California, December 1999.
- [18] H. von Bremen, F. Udawadia, W. Proskurowski, An efficient QR based method for the computation of Lyapunov exponents, *Phys. D* 101 (1997) 1–16.
- [19] F. Udawadia, H. von Bremen, W. Proskurowski, A note on the computation of the largest  $p$  LCEs of discrete dynamical systems, *Appl. Math. Comput.* 114 (1999) 205–214.